Annals of Nuclear Energy 101 (2017) 203–214

Contents lists available at ScienceDirect

Annals of Nuclear Energy

journal homepage: www.elsevier.com/locate/anucene

The homogeneous and Lagrangian tracking approaches of the spray simulation in the containment

Peng Ding [a], Yulan Liu [a,*], Biao Wang [b], Wanai Li [b,*], Jiajun Wang [c]

[a] School of Engineering, Sun Yat-Sen University, Guangzhou, China
[b] Sino-French Institute of Nuclear Engineering and Technology, Sun Yat-Sen University, Zhuhai, China
[c] China Nuclear Power Technology Research Institute, Shenzhen, China

ARTICLE INFO

Article history:
Received 12 May 2016
Received in revised form 12 September 2016
Accepted 25 September 2016
Available online 19 November 2016

Keywords:
Spray simulation
Homogeneous approach
Lagrangian tracking approach

ABSTRACT

The spray system is an emergency containment cooling strategy to depressurize and remove heat in the steam or hydrogen generation scenarios. Different kinds of phenomena including gas-droplets mixing, water vaporization, and steam condensation, are coupled into the complicated flow. The thermal-hydraulic simulation code GASFLOW is widely used and verified in series of containment experiments. Also, a homogeneous spray model which treats the droplets as one species in the gas mixture is incorporated in this code. This paper developed the Lagrangian tracking way for the spray simulation which viewed the droplets as dispersed phase. And in this approach, the interactions for gas-droplets and wall-droplets were considered in all aspects of mass, momentum and energy. The priorities of Lagrangian tracking way over homogeneous way were showed by the TOSQAN 101 and 113 spray benchmarks tests. Detailed comparisons between the two models were concentrated on the condensation-evaporation procedure and gas mixing. All these revealed that the Lagrangian way could predict the phase transition and momentum exchange correctly.

1. Introduction

During the course of a hypothetical severe accident in a Pressurized Water Reactor (PWR), pressurization can be produced or hydrogen can be released in a containment by the loss-of-coolant accident (LOCA) event or loss of power transients. The spray system begins to function to reduce the risk of structural damage or hydrogen explosion. The aim of the containment spray system is to depressurize the containment by steam condensation, cool the containment by droplets evaporation and reduce local extremes of hydrogen concentration by the enhancement of the containment atmosphere mixing (Malet et al., 2011). It is required to study spray procedures to check the feasibility and actual performance.

Many investigations have been made on the spray system both experimentally and theoretically in the last few decades. There were severe early experiments performed in large-scale facilities, NUPEC, CSE and CVTR (Malet et al., 2014; Malet, 2003). Besides, the SARNET spray benchmark based on TOSQAN and MISTRA experiments has been investigated to study the influence of containment sprays on atmosphere behavior (Malet et al., 2011). The TOSQAN 101 and MISTRA MASPn tests were carried out to deal with depressurization by spray which is described as the "thermal-hydraulic part" of spray (Malet et al., 2005). Also, the TOSQAN 113 and MISTRA MARC2b tests were investigated to deal with light gas stratification break-up by spray (Abdo et al., 2006a, b).

The correct numerical calculation of the spray system is a non-trivial thing which deals with the mass, momentum and energy exchange between gas mixture and droplets. As a liquid phase, spray droplets can be described in either Lagrangian or Eulerian method. The Lagrangian framework tracks the droplets as the dispersed phase, while the Eulerian framework regards spray as the continuous phase. All approaches may be necessary during the whole spray simulation. Babić used the droplet-tracking modeling to simulate TOSQAN spray test based on the CFX code (Babić et al., 2009). This model tracked droplets and viewed them as sources or sinks of energy, mass and momentum in the single-phase gaseous field. Analysis of containment spray activation effects on behavior of steam and hydrogen in the Advanced Power Reactor (APR1400) and the CPR 1000 type pressurized water reactor (PWR) have been performed with the GASFLOW code (Kim et al., 2006; Huang et al.,

* Corresponding authors at: School of Engineering, Sun Yat-Sen University, Panyu, Guangzhou 510006, China (Y. Liu). Sino-French Institute of Nuclear Engineering & Technology, Sun Yat-sen University, Tangjiawan, Xiangzhou, Zhuhai 519082, China (W. Li).

E-mail addresses: stslyl@mail.sysu.edu.cn (Y. Liu), liwai@mail.sysu.edu.cn (W. Li).

http://dx.doi.org/10.1016/j.anucene.2016.09.038
0306-4549/

2011; Xiong et al., 2009). The homogeneous two-phase flow model is used with the assumption of thermal non-equilibrium and mechanical equilibrium between the phases. Mimouni developed the two-phase flow model to calculate TOSQAN spray test based on the NEPTUNE_CFD code (Mimouni et al., 2010). This solver is based on the classical two-fluid one pressure approach, including mass, momentum and energy balances for each phase. Malet used a Eulerian-Lagrangian model to simulate the evolution of the helium concentration when the spray was activated (Malet and Huang, 2015). The spray characteristic influence on local light gas mixing was analyzed. Different kinds of approaches are already applied in codes for simulating some spray phenomena to some degree.

The homogeneous model is adopted in two-phase flow for different applications. This model is simple and easy to be incorporated into the basis solver. Moreover, it can capture the main physical phenomena and reveal the basis discipline. The GASFLOW uses it to represent the droplets evaporation and condensation procedure. This paper tries to show the capability of this model and its limits. On the other hand, the Lagrangian tracking method is a more sophisticated approach to simulate the spray. Since a large amount of droplets are tracked in the spray, the particle cloud hypothesis is used in Lagrangian tracking method to improve the calculation efficiency.

There still exist some arguments about the spray depressurization and heat removing roles. The hot containment gas would vaporize the droplets, which decreases the temperature yet increases the pressure inside due to more steam. On the other hand, the saturated steam would condense on the droplets with lower temperature. The overall effect still remains unknown which depends on all kinds of factors including the droplet injection rate and temperature, the concentration for the steam, etc. The spray benchmark TOSQAN 101 is mainly used to study this phase transition procedure. This paper tries to clarify the procedure by using the two models to check what kind of phase change dominates at different times and regions. The spray benchmark TOSQAN 113 test is used to study the gas mixing procedure and to compare the capability of these two models.

2. Computational model

The well-tested CFD code GASFLOW (Travis et al., 1998) is used in this study to provide the basic solver for calculating the transportation of the containment atmosphere which is regarded as the continuous phase or the "carrier fluid". The code solves the unsteady compressible Reynolds-averaged Navier-Stokes(RANS) equations with the finite-volume scheme on the structured 3D meshes. The ICE'd ALE approach is used in this solver that consists of three operating steps (Travis et al., 1998). The first step is an explicit Lagrangian phase for updating the source terms and diffusion terms, the second step is an implicit pressure iteration process to achieve convergence, and the last step is named by "rezone phase" which used an upwind scheme to calculate the convective terms. A homogeneous model is also applied in this code which views droplets as a new species. This model uses the assumption of the mechanical equilibrium and yet allows the mass/heat non-equilibrium between phases, which means droplets have the same velocity as gas and independent temperature. To consider the velocity difference, the Lagrangian tracking way is adopted and described below.

2.1. The homogeneous approach

The homogeneous approach was advanced by Carrier and Marble primarily in the study of particle-laden compressible flow, which is called as "dust gas" (Carrier, 1958; Marble, 1970). This approach considers spray droplets as a component in the continuous phase and yet is thermally independent. The spray droplet has its own diameter, temperature and effective component density. This approach assumes that the particles are sufficiently small that they perfectly follow the gas phase, which means the droplets share the same velocity with the ambient gas. The governing equations of spray models are

- droplet concentration equation

$$\frac{\partial \rho_{h2ol}}{\partial t} + \mathrm{div}(\rho_{h2ol}\mathbf{u}) = S_{\rho,h2ol}. \tag{1}$$

- droplet energy equation

$$\frac{\partial (\rho_{h2ol} e_{h2ol})}{\partial t} + \mathrm{div}(\rho_{h2ol} e_{h2ol}\mathbf{u}) = S_{e,h2ol}. \tag{2}$$

- droplet diameter equation

$$\frac{\partial d}{\partial t} = \langle \mathbf{u}, \nabla d \rangle + \frac{d}{3}\frac{S_{\rho,h2ol}}{\rho_{h2ol}}. \tag{3}$$

where ρ_{h2ol} is the species density of spray droplets in the gas-droplet mixture, $\mathbf{u}$ is the velocity of the mixture, e_{h2ol} is the specific energy of the droplet, and d is the droplet diameter. $S_{\rho,h2ol}$, $S_{e,h2ol}$ are the mass resource and the energy source of the spray respectively which are written as,

$$S_{\rho,h2ol} = h_m A_p \rho_{i,\infty} ln(1 - B_m)/V. \tag{4}$$

$$S_{e,h2ol} = h_e A_p (T_\infty - T_p) - S_{\rho,h2ol} L_{fg}. \tag{5}$$

where $B_m = \frac{y_{h2o,sat} - y_{h2o,\infty}}{1 - y_{h2o,sat}}$ is the mass Spalding number, $y_{h2o,sat}$ and $y_{h2o,\infty}$ are the vapor mass fraction at droplet surface and in the bulk gas respectively. The homogeneous approach uses the temperature of the spray droplet T_p to determine the temperature of the droplet surface. L_{fg} is the latent heat for the droplet, and $A_p = \pi d^2$ is the surface area for the droplet. h_m and h_e are the mass transfer coefficient and heat transfer coefficient respectively which are determined by the Sherwood number Sh and Nusselt number Nu,

$$h_m = \frac{ShD}{d}, h_q = \frac{Nu\lambda}{d} \tag{6}$$

And the non-dimensional numbers are calculated with widely used Ranz and Marshall correlations (Ranz and Marshall, 1952),

$$Sh = 2 + 0.552 \mathrm{Re}_p^{1/2} Sc^{1/3}. \tag{7}$$

$$Nu = 2 + 0.552 \mathrm{Re}_p^{1/2} \mathrm{Pr}^{1/3}. \tag{8}$$

The GASFLOW solver uses the global time step for the transient gas flow which is subject to the Couran-Friedrichs-Lewy (CFL) condition,

$$\Delta t_g = CFL \min(\Delta t_{convection}, \Delta t_{diffusion}). \tag{9}$$

where CFL is chosen to be 1 when not specified. In this equation, the time step is constrained by both convective and diffusion time steps which are defined by

$$\Delta t_{convection} = \frac{1}{4 \max\{\frac{|u_i|}{\Delta x_i}, \frac{|v_i|}{\Delta y_i}, \frac{|w_i|}{\Delta z_i}\}} \tag{10}$$

and

$$\Delta t_{diffusion} = \frac{1/(4\lambda_i)}{\frac{1}{\Delta x_i^2} + \frac{1}{\Delta y_i^2} + \frac{1}{\Delta z_i^2}}, \lambda_i = \max\{D_{eff}, v_{eff}, \frac{k_{eff}}{\rho c_p}\}_i \tag{11}$$

with D_{eff}, v_{eff} and k_{eff} be the effective mass diffusion, viscosity and heat conductivity coefficients respectively. Since the homogeneous model does not introduce any diffusion terms and the convection velocity adopts the gas one, this time step naturally guarantees the stability in solving Eqs. ((1)–(3)).

2.2. The Lagrangian tracking approach

The spray droplets are viewed as the spatially-dispersed phase. Thus, the Lagrangian tracking method is a natural choice to describe the movement of the droplets. Before further description of this model, the requirement and consideration need to clarify first,

(1) This model can simulate large amount of droplets;
(2) Mass, momentum and energy interactions between gas-droplet and gas-wall need taking into account;
(3) Turbulence effect must be considered in droplets movements;
(4) Droplets fragmentation and coalescence are neglected in this paper for simplicity because of their limited effect on phase transition and gas mixing.

For the point (1) above, the particle cloud hypothesis is implemented in the spray model. The assumption is that one particle cloud consists of a number of spray droplets with the same location, diameter, temperature and velocity. At the injection nozzle, the number of particle cloud N_c is evaluated as

$$N_c = \frac{m_{inject}\Delta t_{inject}}{m_c} \tag{12}$$

where m_{inject} is the injection rate from the spray nozzle, m_c is the mass for one group. Δt_{inject} is the time step in the Lagrangian tracking model and is independent of time step for the gas phase. The number of droplets in one group is therefore calculated by

$$K_{c,p} = \frac{m_c}{m_p},\ m_p = \frac{1}{6}\rho_p \pi d^3 \tag{13}$$

where ρ_p is the density of droplet and m_p is the mass of one droplet. Thus K_p relies on the number of particle cloud N_c which is given by code users.

To consider the mass, momentum and energy interactions between gas and droplet, only one droplet is taken to give the balance laws. The droplet velocity $\mathbf{u}_p$ is affected by the drag force $\mathbf{F}_D$, gravity $\mathbf{G}_p$ and buoyancy force $\mathbf{F}_b$. And its equation is given as

$$m_p \frac{d\mathbf{u}_p}{dt} = \mathbf{F}_D + \mathbf{G}_p + \mathbf{F}_b \tag{14}$$

Due to the assumption that the shape of the spray droplet is regarded as the sphere, the drag force is written as

$$\mathbf{F}_D = \frac{1}{2} C_d \rho_g A |\mathbf{u}_g - \mathbf{u}_p|(\mathbf{u}_g - \mathbf{u}_p) \tag{15}$$

where C_d is the particle drag coefficient, ρ_g is gas density, $\mathbf{u}_g$ and $\mathbf{u}_p$ are gas velocity and particle velocity respectively, and $A = \frac{1}{4}\pi d^2$ is the droplet projected area on the relative velocity direction. The particle drag coefficient requires evaluation of the particle Reynolds number Re_p which is written as

$$\mathrm{Re}_p = \frac{\rho_g d|\mathbf{u}_g - \mathbf{u}_p|}{\mu_g}. \tag{16}$$

For $\mathrm{Re}_p > 905.29$, the drag coefficient is calculated from Newton's resistance law which is chosen to be 0.44; for $0.7 < \mathrm{Re}_p \leqslant 905.29$, the coefficient is given by Clift et al. (Clift et al., 2005); for $\mathrm{Re}_p < 0.7$, the coefficient is given by Oseen's law (Oseen, 1910). Thus we have

$$C_d = \begin{cases} \frac{24}{\mathrm{Re}_p}\left(1 + \frac{3}{16}\mathrm{Re}_p\right) & \mathrm{Re}_p \leqslant 0.7 \\ \frac{24}{\mathrm{Re}_p}\left(1 + \frac{1}{6}\mathrm{Re}_p^{2/3}\right) & 0.7 < \mathrm{Re}_p \leqslant 905.29 \\ 0.44 & \mathrm{Re}_p > 905.29 \end{cases}. \tag{17}$$

The gravity force and buoyancy force are combined as

$$\mathbf{G}_p + \mathbf{F}_b = \frac{\pi}{6} d_p^3 \mathbf{g}(\rho_p - \rho_g). \tag{18}$$

The gas velocity in Eq. (15) should take into account of the turbulence effect, i.e.

$$\mathbf{u}_g = \bar{\mathbf{u}}_g + \mathbf{u}'_g. \tag{19}$$

where $\bar{\mathbf{u}}_g$ is time averaged velocity given by GASFLOW solver for the RANS equation, $\mathbf{u}'_g$ is the velocity fluctuation. This fluctuation can be calculated by the discrete random walk model to obtain the particle turbulent dispersion. In the discrete random walk model, the velocity fluctuation follows the Gaussian distribution random presumptively (Gosman and Loannides, 1983) and is written as

$$\mathbf{u}'_g = \left(u'_g, v'_g, w'_g\right), u'_g = v'_g = w'_g = \zeta\sqrt{2k/3} \tag{20}$$

where ζ is normally distributed numbers, and k is the kinetic energy of turbulence.

The standard droplet heat and mass transfer model proposed by Godsave and Spalding is applied to estimate the mass evaporation or condensation rate (Sazhin, 2006). This model is based on the so-called 'corrected spherical symmetry' assumption. The dispersed phase equilibrium is considered in this model and the equations are

$$\frac{dm_p}{dt} = h_m A_p \rho_{i,\infty} ln(1 - B_m). \tag{21}$$

$$m_p c_p \frac{dT_p}{dt} = h_e A_p (T_\infty - T_p) - \frac{dm_p}{dt} L_{fg}. \tag{22}$$

The terms on the right-hand side of Eqs. (21) and (22) follow the same definition as Eqs. (6)–(8). For estimation of the droplet surface temperature T_f and vapor mass fraction y_f, the "1/3 rule" is used to yield the most reliable results,

$$T_f = T_p + \frac{1}{3}(T_\infty - T_p). \tag{23}$$

$$y_f = y_{h2o,sat}(T_f). \tag{24}$$

The mass and energy Eqs. (21) and (22) are coupled and solved implicitly using the Newton iteration method.

The two-way interaction is considered in this paper, thus the influence of continuous phase due to droplets is given as source form in the gas balance equations, i.e.,

$$S_{\rho,h2o} = -\sum_c K_{c,p}\frac{dm_p}{dt}, \tag{25}$$

$$S_{mom} = -\sum_c K_{c,p}\mathbf{F}_D dt, \tag{26}$$

$$S_e = -\sum_c K_{c,p} m_p c_p \frac{dT_p}{dt}. \tag{27}$$

where $K_{c,p}$ is the droplet number of the practical cloud in one particular cell. The summation is cycled for all the particle clouds in one cell.

The implicit algorithm is used to solve the Eqs. (14), (21) and (22). The maximum residuals of the droplet diameter, temperature and velocity are converged to 10^{-5}, 10^{-4} and 10^{-3} respectively. The stable time step of the particle tracking integration is chosen

locally as the element length scale divided by the particle speed to update the particle location, which is given by

$$\Delta t_p = C_{particle} \min\left\{\frac{\Delta x}{u_p}, \frac{\Delta y}{v_p}, \frac{\Delta z}{w_p}\right\}. \quad (28)$$

where $C_{particle}$ is chosen to be 1 when not specified. The final time step for both gas and particle chooses the minimal value of Eqs. (9) and (28), i.e.

$$\Delta t = \min(\Delta t_p, \Delta t_g). \quad (29)$$

2.3. Wall boundary treatment

When spray droplets reach the facility wall or sump, the height and temperature of the film or sump will be changed. The source term of the mass and energy is adopted in the film balance equations to update the height and temperature of the film and sump, which are written as

$$S_{\rho,h2o,film/sump} = \sum_c K_{c,p,film/sump} m_p. \quad (30)$$

$$S_{e,film/sump} = \sum_c K_{c,p,film/sump} m_p e_p(T_p). \quad (31)$$

where $K_{c,p,film/sump}$ is the droplet number of the practical clouds that reach the wall or sump boundary. Due to the limited influence on the mass change of the film and sump, the neglect of droplet splash is reasonable. Besides, the movement of the film is not considered in this paper for simplicity because of a small fraction droplets reached wall other than the vessel bottom or sump. As for the heat and mass transfer in the film and sump, the modified Reynolds analogy model combining with Chilton-Colburn empirical analogy is applied. The detail information about the spray-sump interaction in the homogeneous approach and validations are given in (Travis et al., 1998).

3. The experiments and GASFLOW input

3.1. TOSQAN 101

TOSQAN 101, originally initiated by FZK and IRSN in March 2003, is the spray benchmark to validate the spray "thermal-hydraulic part" under typical conditions of the hypothetical nuclear reactor accident (Malet et al., 2011; Porcheron et al., 2007). The TOSQAN facility geometry and spray injection location are presented in Fig. 1. The TOSQAN facility is a closed cylindrical vessel with 7 m^3 volume, 1.5 m diameter and 4.8 m height. The temperature of the vessel wall is controlled by oil circulation. The spray nozzle is located at 70 cm from the top of the facility on the vessel axis. A steel sump with 0.68 m diameter is attached at the bottom of the vessel. There are many available instrumentations applied in TOSQAN facility. Gas temperature is measured by thermocouples. Spray droplet and gas velocities are measured with particle image velocimetry (PIV) and laser Doppler velocimetry (LDV). Gas concentrations are measured with a mass spectrometer and spontaneous Raman scattering spectroscopy (SRS). Detailed descriptions of the instrumentation position can be found (Porcheron et al., 2007).

At the beginning of TOSQAN 101, superheated steam is injected into the vessel until the total pressure reaches to 2.5 bars. The temperature of the vessel walls is kept very high. After stopping the steam injection, the spray starts at 25 °C droplet temperature and 30 g/s mass flow rate. The test initial condition is presented in Table 1.

The thermostatically controlled wall temperature of the vessel is shown in Table 2. During the experiment TOSQAN 101, the wall temperature is controlled by the circulation of heating oil through different wall sections. Also, the temperature of the sump is determined by the wall temperature.

Due to the upward steam injection at 2.1 m of the vessel before the spray activation, there is a strong atmosphere stratification occurred in the vessel. The initial steam distribution in the vertical direction is shown in Table 3. The parameters of spray in the TOSQAN 101 test are shown in Tables 4 and 5. These details of the TOSQAN 101 were available in the SARNET benchmark exercise (Malet et al., 2011).

Table 1
Initial conditions of integral parameters for the simulation of TOSQAN 101.

Mean gas temperature out of the spray zone	Mean gas temperature in the spray zone	Total pressure	Initial gas composition (from mass balance)
131.1 °C	131.0 °C	2.5 bar	Air: 213 mol; Steam: 308 mol;

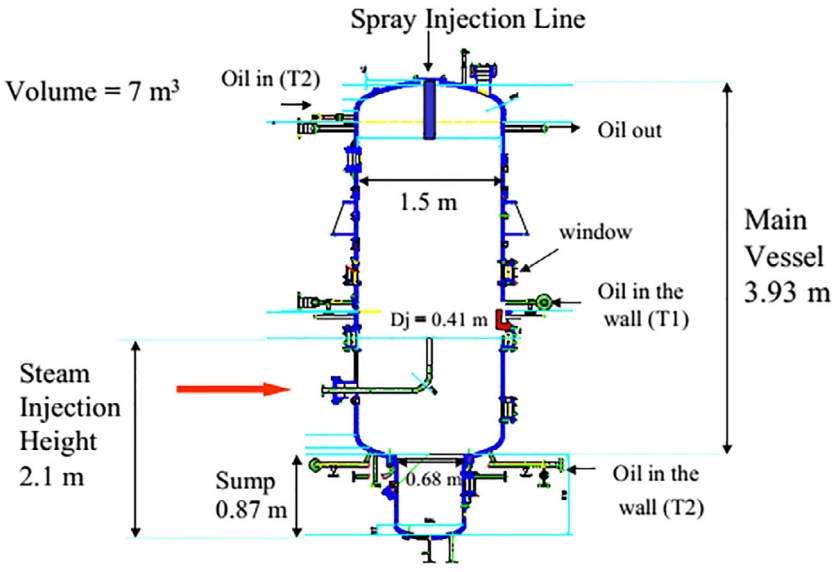

Fig. 1. Schematic view of the TOSQAN vessel (Malet et al., 2011).

Table 2
Prescribed variation of wall temperatures for the simulation of TOSQAN 101 spray test.

Time (s)	Lower wall temperature (°C)	Middle wall temperature (°C)	Upper wall temperature (°C)
0–102	121.4	121.6	121.3
102–300	120.8	120.4	120.3
300–601	120.3	120.0	119.4
601 s–end	119.3	120.1	115.4

Table 3
Initial steam distribution for the simulation of TOSQAN 101.

Elevation(m)	Steam molar fraction
0.871	0.1
2.25	0.7
4.8	0.7

Table 4
Spray characteristics in the experiment TOSQAN 101.

Spray flow-rate	Spray angle	Spray injection height	Initial droplet size	Initial droplet velocity
29.96 g/s	55°	0.65 m	146 μm	10 m/s

Table 5
The temperature of the spray for the simulation of TOSQAN 101.

Time (s)	The temperature of the spray (°C)
0–120	119.0–22.1, linear function of time
120–1500	22.1–27.7, linear function of time

There are three phases during the test (Lemaitre et al., 2005). Phase 1 is the initial droplet evaporation phase. Strong evaporation of droplets occurred in the first 100 s due to high initial temperature (about 130 °C). Phase 2 is the condensation and mixing phase for the next 200 s. During the transition to the atmosphere saturation state, the steam condensation appears on droplets and mixture is cooling due to convection heat transfer to droplets. Phase 3 is condensation phase. The gas temperature and steam mass decrease slowly during the next 3000 s.

3.2. TOSQAN 113

Before the TOSQAN 113 test, the compressed air is injected into the facility to remove helium and steam and the test condition reaches a thermal steady state. The helium, which is used to replace the flammable hydrogen, is injected into the facility at about 1 g/s mass flow rate until the mean pressure reaches 2 bar. The helium injection nozzle is situated on the top of the dome, with 13 mm diameter. There is a delay of 400 s before the spray injection in order to establish the helium initial stratification. The initial conditions of the mean gas temperature and the helium are given in Table 6. Then, the spray starts with a mass flow-rate of 30 g/s and a steady state is reached at the end of test 113. The characteristics of spray for this experiment are given in Table 7. Besides, the wall of the vessel is insulated in this test. More information about this test can be found (Malet et al., 2011).

4. Result and discussion

The numerical simulation presented in this section is used for the evaluation of the homogeneous and Lagrangian tracking approaches in the spray calculation in the small-scale containment. In the spray simulation cases, the TOSQAN facility was modeled with the three-dimensional mesh, which contained 14040 elements shown in Fig. 2. All boundaries were treated as walls with the specific temperature which are given in Table 2 and the wall function was applied to the boundary layers. The adaptive time stepping scheme was used in these cases with time step between 10^{-5} s and 10^{-3} s. These settings can ensure that the maximum residuals of pressure value converged to 10^{-6} in every step. The main purpose of TOSQAN spray test is the investigation on the break-up of the stratified atmosphere and containment depressurization by mass, momentum and heat transfer by spray droplets. To satisfy the experiment demands in simulations, the evaporation and condensation models were considered on the surface of sumps and walls. The simulation condition is the same for the two spray models except for the spray injection way.

Table 6
Initial conditions before spray injection in TOSQAN 113 test.

Z (from the bottom, m)	Helium concentration (%)	Mean gas temperature (°C)
Z13 = 3.93	99.0	32.8
Z11 = 2.13	85.8	36.9
Z10 = 2.80; Z9 = 2.67	47.6 (Z10)	34.7 (Z9)
Z5 = 1.90; Z6 = 2.04	2.3 (Z5)	30.1 (Z6)
Z1 = 0.87; Z2 = 1.20	1.9 (Z1)	28.7 (Z2)

Table 7
Spray characteristics in the experiment TOSQAN 113.

Spray flow-rate	Spray angle	Spray injection height	Initial droplet size	Initial droplet velocity
29.96 g/s	55°	0.65 m	135 μm	10 m/s

4.1. TOSQAN 101

The grid and time convergence study on this test is conducted in terms of the mean pressure. Three cases are considered in the calculation. The first one is the standard case with the mesh shown in Fig. 2 and $C_{particle} = 1$ for the Lagrangian time step, the second one uses a fine mesh with half the grid size on every dimension and $C_{particle} = 1$, and the third one uses the fine mesh and $C_{particle} = 0.5$. The homogenous model is only valid for the former two cases without $C_{particle}$ parameter. The measured results for the time histories of mean pressure are shown in Fig. 3. The cases with fine mesh or smaller time step all come quite close the standard case, which indicates the standard case is sufficient to compute the TOSQAN 101 case.

The comparison of the total gas mole number between calculated data and experimental data is presented in Fig. 4. The total gas mole number is determined by the total mass of the mixture in the facility which consists of air and vapor. The time evolution of the gas mole number is a specific parameter to represent the process of spray droplet evaporation and steam condensation. The Lagrangian tracking model can accurately predict the gas mole number for the whole time while the homogeneous model seems to under-estimate it after 200 s.

The time evolution comparison of the mean temperature in the facility is shown in Fig. 5. During the first 100 s, the temperature with Lagrangian tracking approach decreases rapidly for the sump and spray evaporation is over-estimated due to high temperature. As we know, the main aim of the TOSQAN 101 spray test is to study atmosphere depressurization during the spray activation. Fig. 6

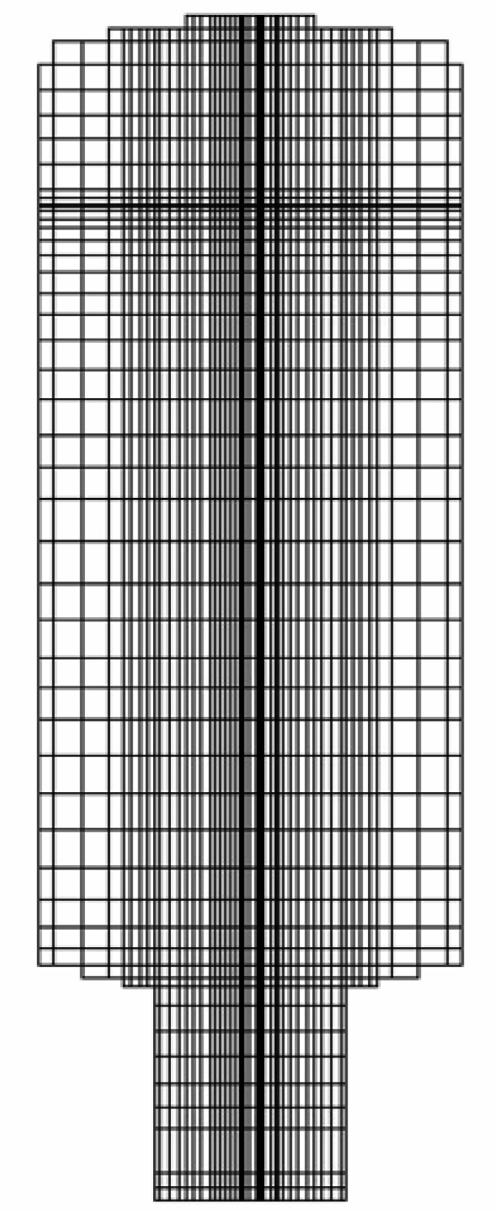

Fig. 2. The mesh of the TOSQAN vessel in the simulation.

shows the comparison of calculated average pressure and measured pressure. From the comparison in the figure, the Lagrangian tracking approach predicts the pressure more accurately than

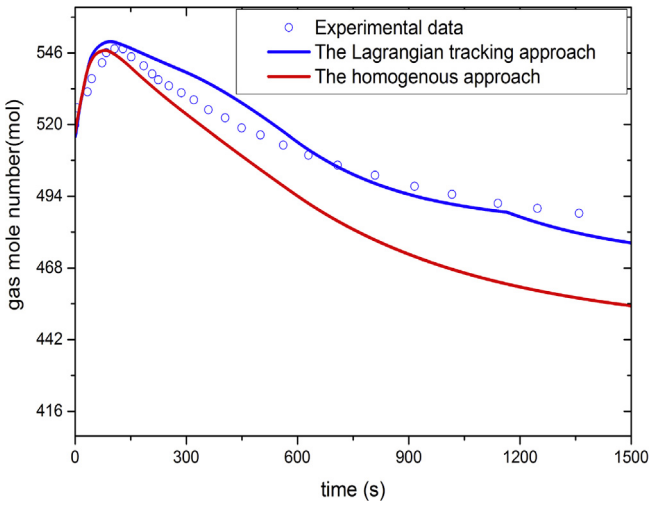

Fig. 4. The comparison of gas moles (air and vapor) between calculated data and experimental data in TOSQAN 101 simulation.

homogeneous method. During the first 100 s, the pressure increases also due to evaporation from the sump. During the next 200 s, Lagrangian tracking approach over-predict a bit the pressure due to over-estimation in the sump evaporation. However, the simulation has a good agreement with measured data with spray injection.

The homogeneous model gives a lower gas moles, temperature and pressure than the Lagrangian approach. The main difference between the two approaches would be the transportation of the droplets. The homogeneous model lack of momentum interaction would give a weak gas mixing. Also, the cause for the depressurization and heat removing process also needs a clear explanation.

Fig. 7 shows the diameter evolution of spray droplets between the homogeneous and Lagrangian tracking approaches. Without considering the drag force between gas and droplets, the droplets with homogeneous model fall faster than that with Lagrangian tracking model, which can be validated from the top figure of Fig. 6. The size of the droplet with the homogeneous model is smaller than that with a Lagrangian tracking model for the condensation reason and will be discussed in the next paragraph. For the right figures using Lagrangian tracking model, the droplets with larger diameter distribute on the external edge of the spray cone zone since the droplets with the smaller diameter are easier affected by the gas moving. The gas mixing causes a circulation as depicted on the bottom of Fig. 6. In the homogeneous model, the droplets movement adopts the gas velocity and can be easier to carry by the gas. Thus the spatial distribution of the droplets

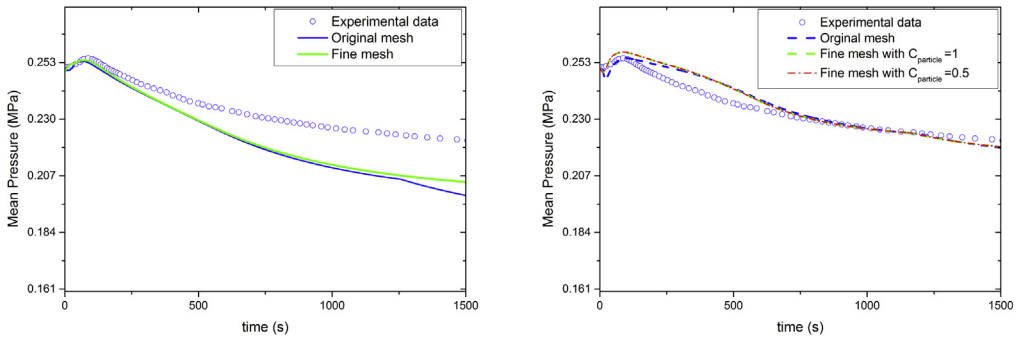

Fig. 3. Time history of the mean pressure for TOSQAN 101 simulation by the homogenous approach (left) and the Lagrangian tracking approach (right) with different meshes and $C_{particle}$.

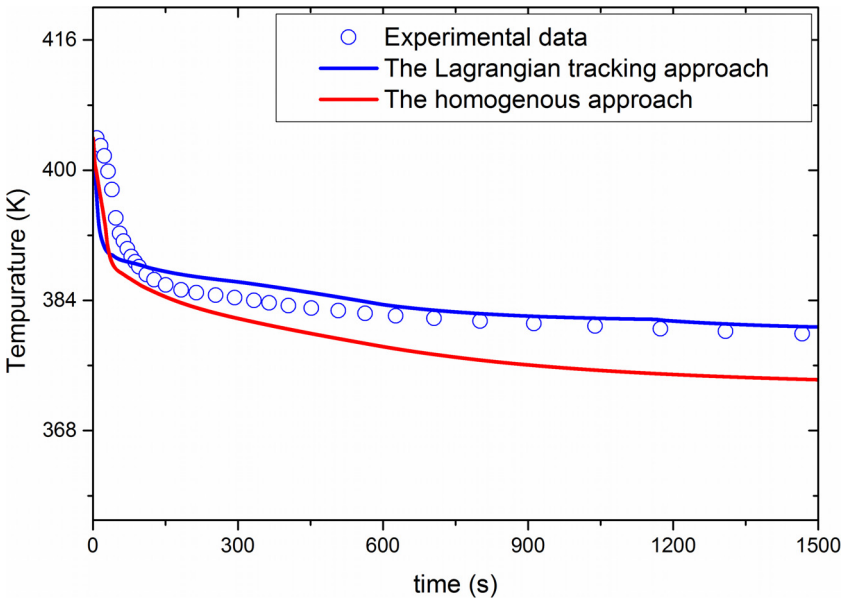

Fig. 5. The comparison of whole global mean temperature time evolution between calculated data and experimental data in TOSQAN 101 simulation.

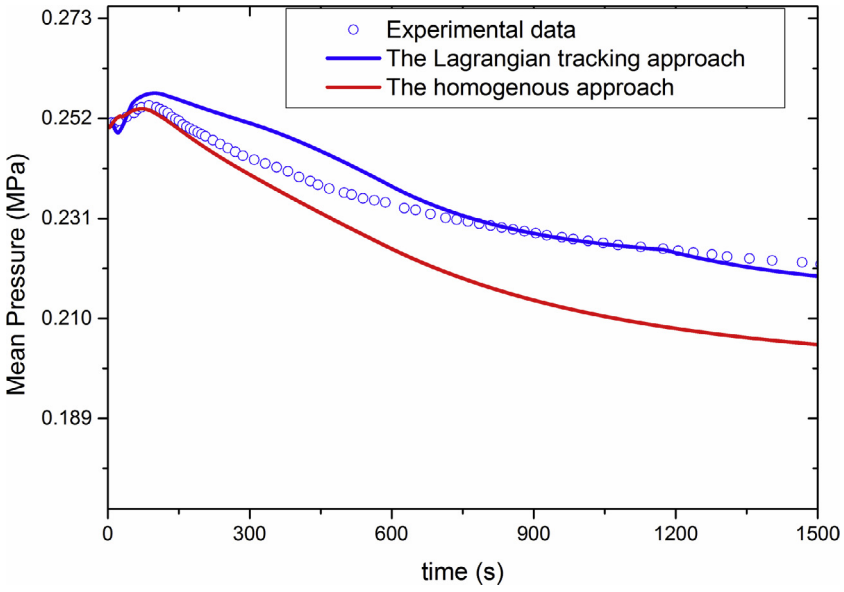

Fig. 6. The mean pressure evolution between calculated data and experimental data in the TOSQAN 101 simulation.

is much wider in the homogeneous model than that in the Lagrangian model.

Fig. 8 shows the comparison of the spray condensation and evaporation rate in the TOSQAN 101 calculation. In the figure, negative values mean condensation, positive values mean evaporation and 0 means no phase change. The top two subfigures show that the spray evaporation region is around the spray nozzle in both approaches at the beginning of spray injection. The spray droplets temperature is high in the first phase of the test and the saturated steam density is higher than the local steam density around the spray droplets. Thus spray evaporation contributes to the main phase transition in the first phase. For the second and third phases, the spray droplet temperature is much lower than the ambient gas according to Table 4. Thus spray condensation takes the main phase transition, which can be verified from the middle and bottom figures. These results coincide with Figs. 4 and 6 that pressure and gas mole number increase at first 100 s and decrease afterward.

However, there is a large discrepancy on condensation regions for these two models for the second and third stages. As depicted in Fig. 7 with the homogeneous model, the droplets can be transported all around the facility and the diameter gets smaller at regions away from the central line. These lead to the condensation occurrences in the whole containment except for the regions close to the hot wall in the left figures of Fig. 8. And the condensation rate becomes weaker away from the nozzle and the central line. The too large condensation region would lead to over-condensation which reflects on Figs. 4–6 that homogenous model predicts lower values for gas mole number, pressure and temperature.

The right-hand-side middle and bottom figures of Fig. 8 with the Lagrangian approach show that the steam condenses at a large

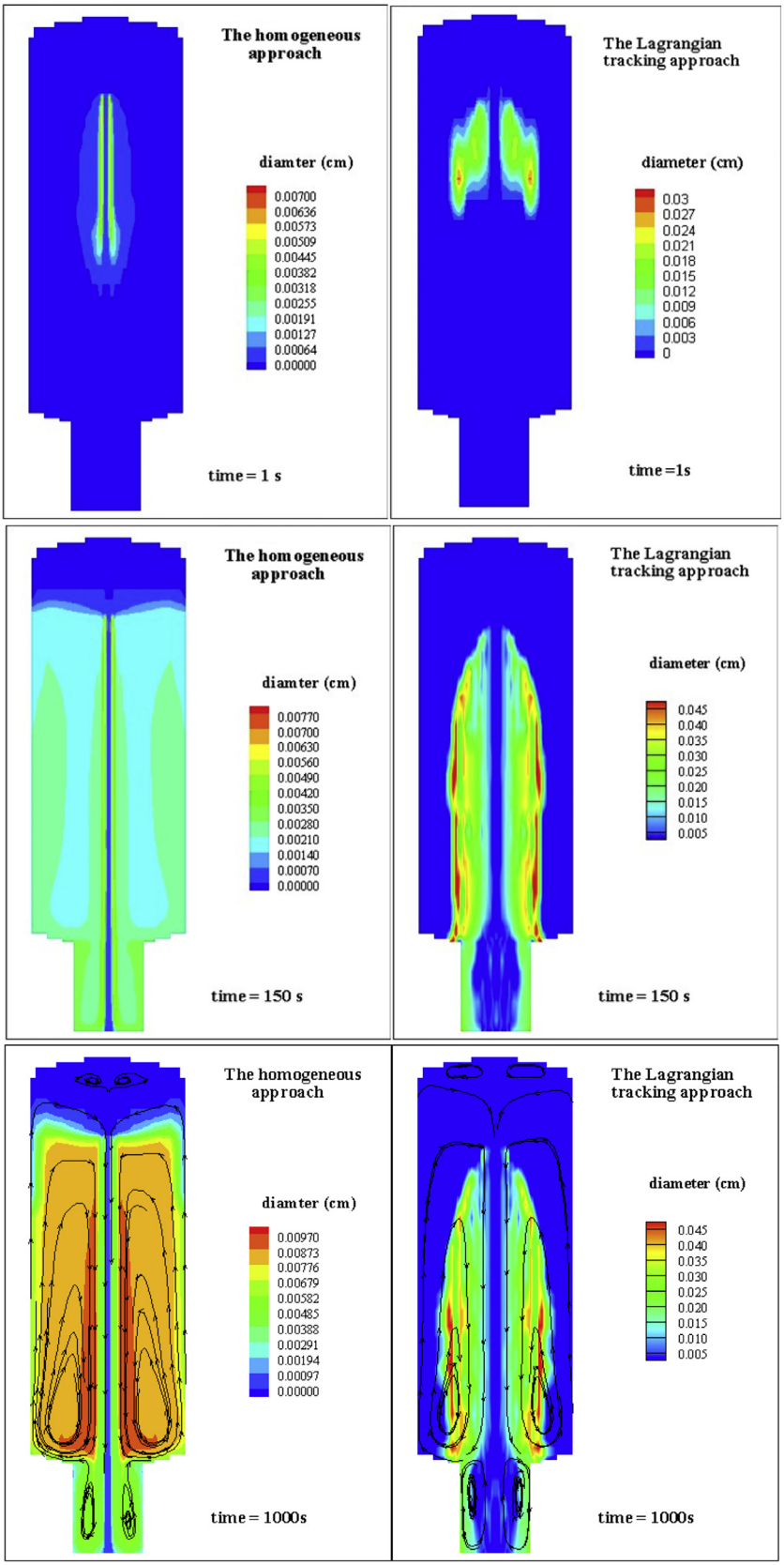

Fig. 7. The comparison of the spray diameter between the homogeneous approaches (left) and Lagrangian tracking approaches (right) at 1 s, 150 s and 1000 s in the TOSQAN 101 simulation.

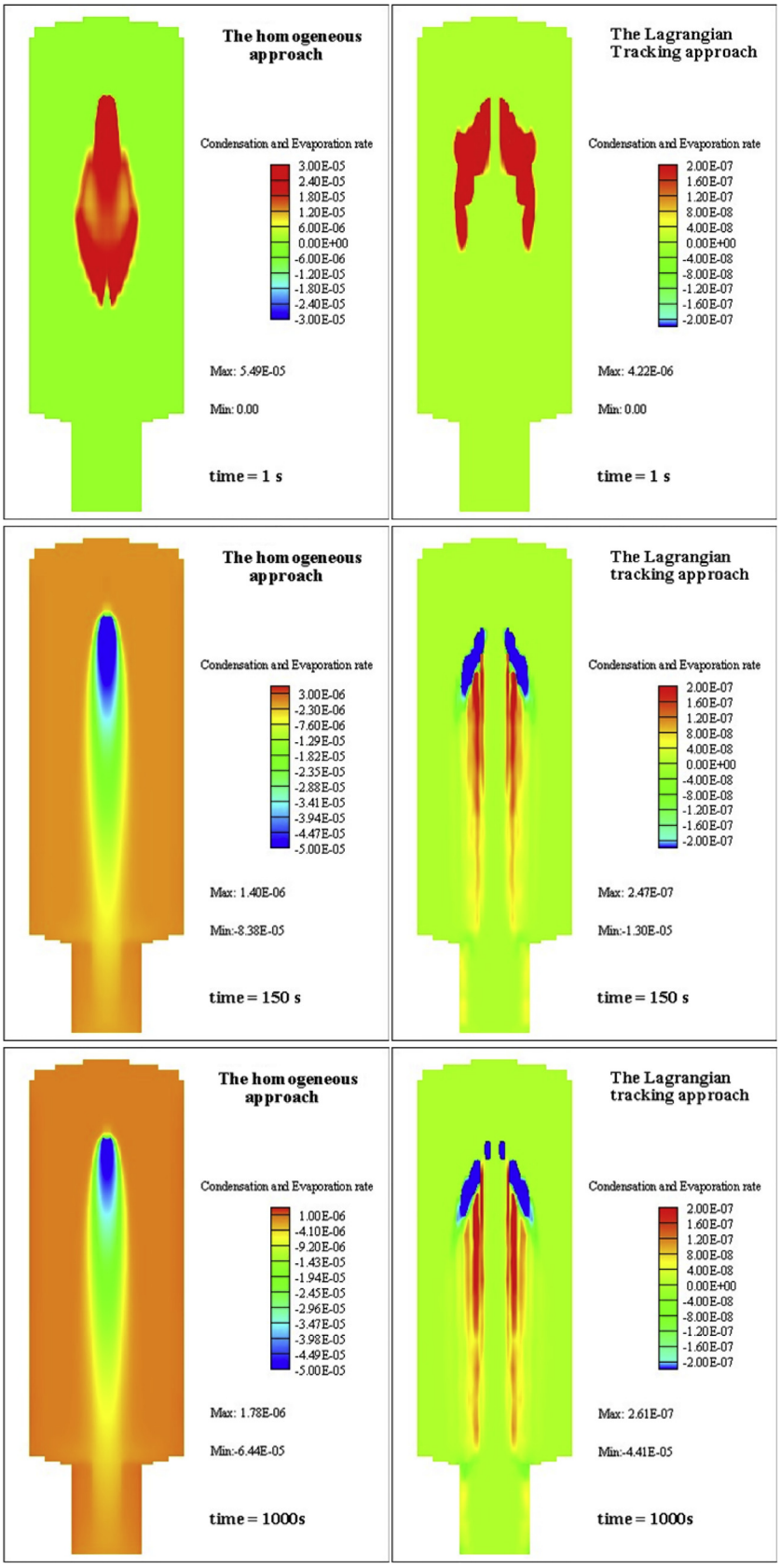

Fig. 8. Comparisons of the condensation and evaporation rate (g/(s cm^3)) between the homogeneous and Lagrangian tracking approaches at 1 s, 150 s and 1000 s in the TOSQAN 101 simulation.

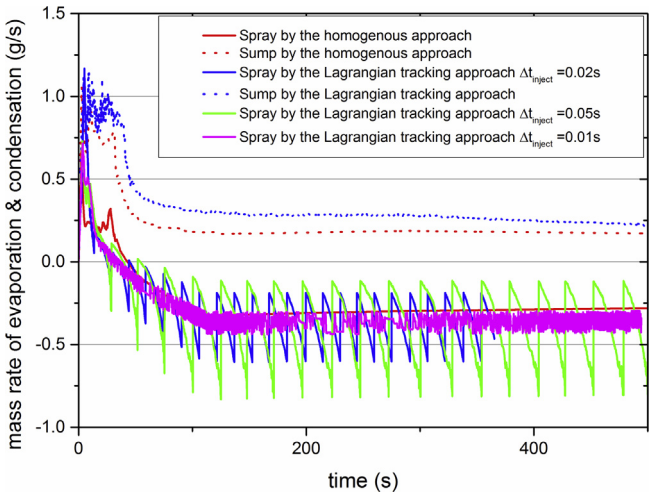

Fig. 9. The mass rate evolution of evaporation and condensation by the spray and sump with the two methods.

rate right under the nozzle for about 0.5 m height, and then droplets evaporate at a rather low rate when falling down. Although the evaporation covers much larger area than the condensation zone, the net mass rate for spray phase change shown in Fig. 9 proves that the condensation plays the leading role.

Moreover, the distribution of condensation and evaporation for the Lagrangian model can be further verified from another side. First, we track the diameter changing process for every class of the droplets. The four classes with different initial diameters calculated with the Lagrangian approach are shown on the left of Fig. 10. From the figure, the diameters of four classes all increase quickly after coming out of the spray nozzle which corresponds to the condensation process shown in the right figures of Fig. 8. And then the diameter with larger initial diameter decreases slowly during the evaporation process. Even for droplets with the smallest initial diameter, the evaporation would not be sufficient to vaporize them back to the initial size. This means condensation mass rate in the shorter time is larger than the evaporation mass rate in the longer time. Also, the droplet temperature in the vertical direction is compared to the experimental data and reference (Babić et al., 2009), as shown on the right of Fig. 10. From the spray nozzle z = 4.0 to z = 2.0, the temperature of different sizes quickly increases to a high value due to condensation, and then reaches a quasi-steady state Due to the fast falling speed of droplets and the decreasing

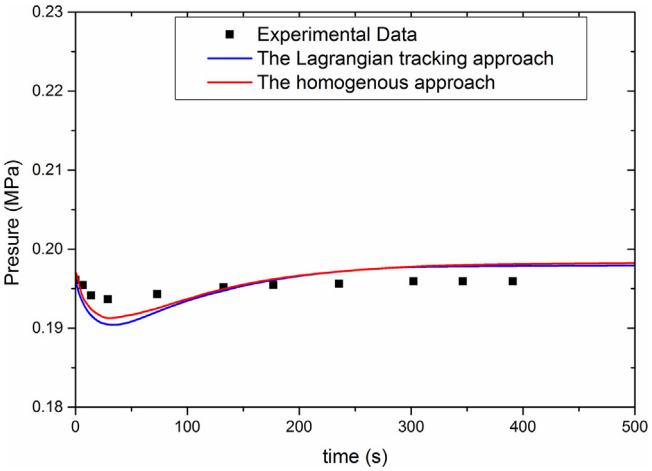

Fig. 12. The mean pressure evolution between calculated data and experimental data in the TOSQAN 113 simulation.

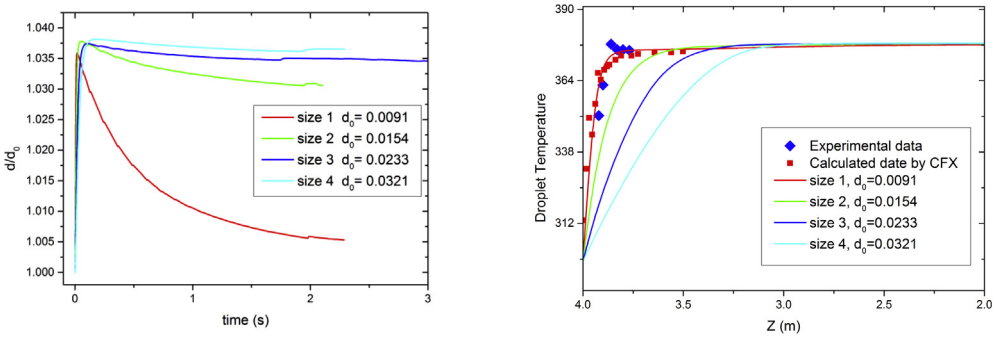

Fig. 10. The diameter evolution (left) of the spray droplet and the droplet temperature (right) with different sizes at 1000 s.

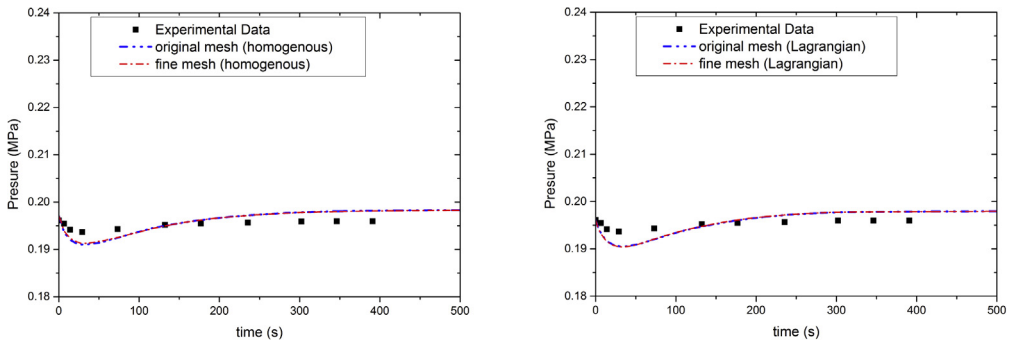

Fig. 11. Time history of the mean pressure for TOSQAN 113 simulation by the Homogenous approach (left) and the Lagrangian tracking approach (right) with different meshes.

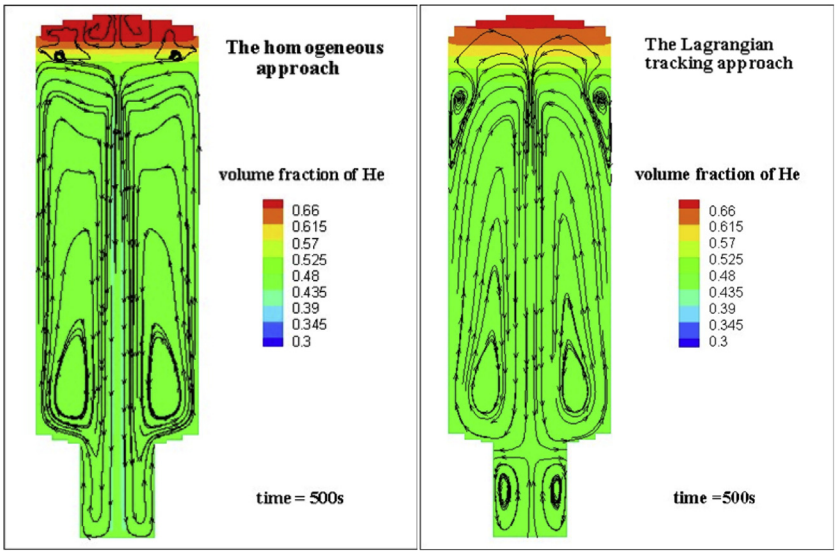

Fig. 13. The stream-lines with the homogeneous approach (left) and the Lagrangian tracking approach (right) in the TOSQAN 113 simulation at 500 s.

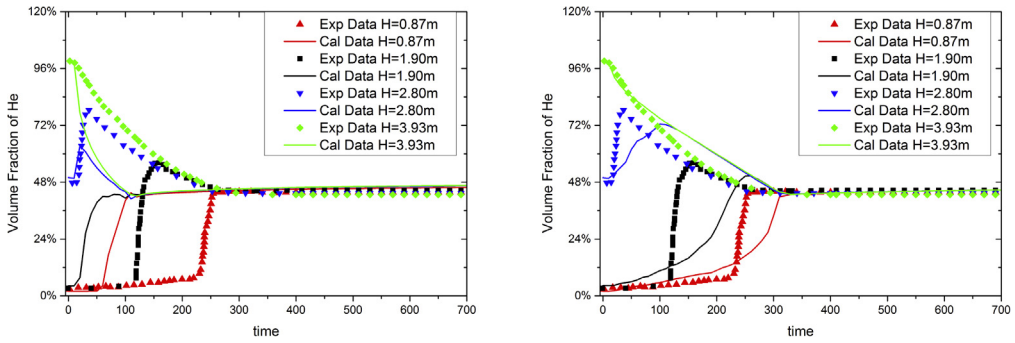

Fig. 14. The helium volume fraction evolution between experimental data and calculated data using the homogeneous (left) and the Lagrangian (right) models in the TOSQAN 113 simulation at different heights.

temperature of the ambient gas, the quasi-steady state can allow a low evaporation rate.

4.2. TOSQAN 113

The main aim of the TOSQAN 113 spray test is to study the gas stratification due to the spray activation with minor heat and mass exchange between gas and droplets. Before the spray activation, the injected helium is stratified in the air-helium mixture. Then the gas mixture is entrained by the spray. During the experiment, it takes about 250 s for the transition from the beginning of spray injection to fully global mixing atmosphere. The key for the calculation would lie in the momentum interaction between the spray and gas mixture.

The grid and time convergence study are also performed firstly with the homogeneous model and Lagrangian tracking model. The calculated mean pressure with respect to time history is shown in Fig. 11, which illustrates the mesh and time step are sufficient in this case.

Fig. 12 shows the comparison of the average pressure evolution in both approaches during the first 400 s of the TOSQAN 113 test. The results show a good agreement in global pressure between calculation and measurement data in spite of the difference of the initial pressure. The decrease of the pressure at the beginning is due to the spray evaporation. Then the pressure increase again caused by the increasing of steam mass. The global pressure is predicted slightly higher than experimental data. The minor change also confirms that spray phase change is not important in this test.

The lack of momentum interaction in the homogeneous model would give an inactive gas mixing during the spray injection. It can be verified from Fig. 13 that the helium concentration with homogeneous model remains high in the doom at 500 s. Whereas for the Lagrangian tracking model, the strongly gas-droplet mixing allows the helium to transport from high concentration area to the low one. The large vortex lies from top to bottom even cause the secondary flow in the upper left and right side. This is also the one application of spray which lowers the concentration of the flammable gas and reduces the risk of explosion.

Fig. 14 shows the comparison of the helium volume fraction between calculated and measured data at the heights of 0.87 m, 1.90 m, 2.80 m and 3.93 m. At 3.93 m height, the helium volume fraction directly decreases due to the enhancement of gas mixing by spray. Comparing to the homogeneous model, the Lagrangian tracking model comes much closer to the experimental data and less time to achieve the full mixing state. Also for other heights the Lagrangian tracking model needs less time to come to the experimental data.

5. Conclusion

This work investigated the containment spray simulation by comparison with the homogeneous and Lagrangian tracking

approaches based on GASFLOW code. The containment atmosphere regarded as the continuous phase is solved by ICE'd-ALE numerical scheme. Two spray experiments, performed in the TOSQAN facility, are chosen to simulate and analyze the spray effect in the containment by two methods. The TOSQAN 101 and TOSQAN 113 spray tests force on depressurization and light gas stratification break-up respectively. A three-dimensional model of the TOSQAN facility is built on GASFLOW code and the spray model is developed under both the homogeneous and Lagrangian tracking framework. Both homogeneous and Lagrangian tracking approaches consider the heat and mass transfer of spray. The homogeneous approach assumes the mechanical equilibrium and makes the implementation simple. The Lagrangian tracking approach considers the spray-gas and spray-wall momentum interactions. The comparisons of the calculated data and experimental data, including the global pressure, temperature and gas volume fraction, show much better agreements with the Lagrangian tracking approach than that with the homogeneous approach. Also, the condensation and evaporation mass rate and regions with Lagrangian approach reveal that condensation is the main reason for the depressurization process.

Acknowledgments

The authors are grateful to the anonymous reviewers for their valuable suggestions and improvements. The work is financially supported by the National Natural Science Foundation of China (No. 11572355 and 10572155), and the IFCEN-CNPRI cooperation (No. 20154500071020018 and 20164500071010005).

References

Abdo, D., Tomassian, R., Brinster, J., Roumier, D., Tkatschenko, I., Widloecher, J.L., 2006a, M5-MASP MISTRA experimental results: Rapport DM2S.

Abdo, D., Tomassian, R., Brinster, J., Roumier, D., Tkatschenko, I., Widloecher, J.L. 2006b. MISTRA Tests MARC2–MARC2B: Air-Helium-Nitrogen Stratification, Effect of Spray on Buoyant Gas Stratification, Report DM2S, SFME/LTMF/RT/05-043/A, Commissariat à l'Energie Atomique-CEA, Saclay, France.

Babić, M., Kljenak, I., Mavko, B., 2009. Simulations of TOSQAN containment spray tests with combined Eulerian CFD and droplet-tracking modelling. Nucl. Eng. Des. 239, 708–721.

Carrier, G.F., 1958. Shock waves in a dusty gas. J. Fluid Mech. 4, 376–382.

Clift, R., Grace, J.R., Weber, M.E., 2005. Bubbles, Drops, and Particles. Courier Corporation.

Gosman, A.D., Loannides, E., 1983. Aspects of computer simulation of liquid-fueled combustors. Journal of Energy 7, 482–490.

Huang, X.G., Yang, Y.H., Cheng, X., Al-Hawshabi, N.H.A., Casey, S.P., 2011. Effect of spray on performance of the hydrogen mitigation system during LB-LOCA for CPR1000 NPP. Ann. Nucl. Energy 38, 1743–1750.

Kim, J., Lee, U., Hong, S., Kim, S., Kim, H., 2006. Spray effect on the behavior of hydrogen during severe accidents by a loss-of-coolant in the APR1400 containment. Int. Commun. Heat Mass Transfer 33, 1207–1216.

Lemaitre, P., Nuboer, A., Porcheron, E., 2005. TOSQAN Experimental Report-Spray Test 101, DSU/SERAC/LECEV/05–11. Institut de Radioprotection et de Surete Nucleaire, Saclay, France.

Malet, J., 2003, Presentation of the tests matrix for the TOSQAN facility Spray Program, Technical Report DSU/SERAC/LEMAC/03-06.

Malet, J., Blumenfeld, L., Arndt, S., Babic, M., Bentaib, A., Dabbene, F., Kostka, P., Mimouni, S., Movahed, M., Paci, S., 2011. Sprays in containment: final results of the SARNET spray benchmark. Nucl. Eng. Des. 241, 2162–2171.

Malet, J., Lemaitre, P., Porcheron, E., Vendel, J., Bentaib, A., Plumecocq, W., Dumay, F., Chin, Y.C., Krause, M., Blumenfled, L., 2005. Modelling of sprays in containment applications: results of the TOSQAN spray benchmark (Test 101). In: Proceedings of The First European Review Meeting on Severe Accident Research, ERSMAR-2005, Aix-en-Provence, France.

Malet, J., Parduba, Z., Mimouni, S., Travis, J., 2014. Achievements of spray activities in nuclear reactor containments during the last decade. Ann. Nucl. Energy 74, 134–142.

Malet, J., Huang, X., 2015. Influence of spray characteristics on local light gas mixing in nuclear containment reactor applications. Comput. Fluids 107, 11–24.

Marble, F.E., 1970. Dynamics of dusty gases. Annu. Rev. Fluid Mech. 2, 397–446.

Mimouni, S., Lamy, J., Lavieville, J., Guieu, S., Martin, M., 2010. Modelling of sprays in containment applications with a CMFD code. Nucl. Eng. Des. 240, 2260–2270.

Porcheron, E., Lemaitre, P., Nuboer, A., Rochas, V., Vendel, J., 2007. Experimental investigation in the TOSQAN facility of heat and mass transfers in a spray for containment application. Nucl. Eng. Des. 237, 1862–1871.

Ranz, W.E., Marshall, W.R., 1952. Evaporation from drops. Chem. Eng. Prog. 48, 141–146.

Sazhin, S.S., 2006. Advanced models of fuel droplet heating and evaporation. Prog. Energy Combust. Sci. 32, 162–214.

Travis, J.R., Spore, J.W., Royl, P., Lam, K.L., Wilson, T.L., Müller, C., Necker, G.A., Nichols, B.D., Redlinger, R., 1998. GASFLOW: a computational fluid dynamics code for gases, aerosols and combustion: FZKA-5994 Vol I-III.

Oseen, C.W., 1910. Über die Stoke'sche Formel und über eine verwandte Aufgabe in derHydrodynamik. Ark. f. Nat. Astr. och Fys. 6, 29.

Xiong, J., Yang, Y., Cheng, X., 2009. CFD application to hydrogen risk analysis and PAR qualification. Science and Technology of Nuclear Installations 2009, 10.